SUMO User Conference 2026

TIBconferencesession

TIB-OP will set DOI with \TIBdoi

Submitted: 1970-01-01

Radar-Based Evaluation of Car-Following Behavior and Fuel Consumption Across Vehicle Categories in SUMO

Calibrating CF Model Parameters

Mahdi Al Abdraboh[1] [https://orcid.org/0009-0001-4906-297X],
Joshua Bittle[1] [https://orcid.org/0000-0003-4524-3316]

[1]University of Alabama, Tuscaloosa, Alabama, USA

Abstract: This study evaluates how well the Intelligent Driver Model (IDM) reproduces observed leader–follower behavior across vehicle categories and how these behavioral differences influence PHEMlight fuel-consumption estimates in SUMO. The analysis uses fused roadside radar trajectories collected along a 1.5 km signalized arterial corridor and classifies follower vehicles into four categories using radar-reported length: Cars, SUVs, light-duty Trucks, and heavy-duty on-highway trucks (Class-8 in U.S.) vehicles. Measured leader trajectories are replayed in SUMO via TraCI, while followers are simulated using IDM. Default parameters and parameters calibrated with a trajectory-level objective in spacing, velocity, and acceleration are compared using RMSE in spacing, velocity, and acceleration. Calibration reduces RMSE across all categories, with the largest reductions in spacing, but Class-8 trajectories retain higher reproduction error than the light-duty categories. A focused Class-8 analysis shows that erroneously simulating the same Class-8 leader–follower trajectories as `vClass` passenger increases uncalibrated spacing and acceleration error relative to the Class-8 (`vClass` trailer) representation, while calibration eliminates the difference between the two representations. PHEMlight fuel-consumption medians decrease after calibration for each vehicle category, with the largest absolute reduction observed for Class-8 vehicles. These results highlight the importance of category-aware behavioral modeling when microsimulation outputs are used for energy and emissions assessment in mixed traffic.

Keywords: traffic microsimulation, car-following models, roadside radar, SUMO, vehicle classification, fuel consumption

1 Introduction

Traffic microsimulation is widely used to study driving behavior, vehicle energy use, emissions, and network performance [1]–[3]. The reliability of these analyses depends on how well the underlying models reflect real-world vehicle motion. Car-following (CF)

models are especially critical because they govern how vehicles respond to one another in the traffic stream and directly shape speed and acceleration profiles [4]. As microsimulation is increasingly applied in environmental assessment and operational planning, there is growing interest in whether these models adequately represent differences in vehicle types and following behavior. This is particularly important for fuel estimation, since acceleration capability and spacing behavior vary substantially across vehicle classes and influence energy use.

Many microsimulation studies continue to rely on calibration using network-level measures such as flow, density, or average segment speeds. Although these metrics are useful, they do not guarantee that simulated leader–follower interactions resemble real trajectories [5]. Prior work has shown that models calibrated only to macroscopic indicators may reproduce aggregate performance while generating unrealistic following behavior at the trajectory level [6]. This limitation has motivated the use of trajectory-based calibration whenever high-resolution data are available. Such detail is especially important for fuel and emissions modeling, because relatively small differences in speed variability and acceleration can produce large differences in predicted energy use [2]. Recent advances in roadside radar sensing have helped address historical data limitations. In particular, Schrader et al. developed a fused radar dataset for a 1.5 km urban corridor that provides continuous, lane-aligned leader–follower trajectories and enables calibration and evaluation directly within SUMO [7].

Despite these advances, prior trajectory-based calibration studies have generally evaluated car-following behavior in aggregate, with limited attention to how performance varies across vehicle types. Empirical trajectory studies indicate that heavy vehicles operate with lower acceleration levels and longer time headways than passenger cars, reflecting more conservative following behavior [8]. These differences affect how disturbances propagate through traffic and can alter vehicle power demand and fuel use, particularly in mixed traffic streams [9]. If CF models do not reproduce these category-specific patterns, fuel and emissions estimates derived from microsimulation may be systematically biased. This concern is especially relevant on corridors with substantial heavy-truck activity, such as freight and port-access routes [10].

This study addresses this gap by explicitly evaluating car-following behavior and fuel-consumption estimates across four vehicle categories: Cars, SUVs, light-duty Trucks, and Class-8 heavy trucks. Here, Class-8 refers to the U.S. heavy-duty truck classification and represents on-highway heavy trucks with trailers in the SUMO simulations. Building on the radar-based calibration framework of [7], measured leader trajectories are replayed in SUMO while follower vehicles are simulated using the Intelligent Driver Model (IDM). Model performance is evaluated using trajectory-level metrics in spacing, speed, and acceleration, and fuel consumption is estimated using the PHEMlight emissions model within SUMO. Applying this framework consistently across vehicle categories enables direct assessment of how behavioral assumptions and calibration influence predicted fuel consumption.

A key contribution of this work is the focused treatment of Class-8 vehicles within the calibration and evaluation framework. By isolating heavy-truck trajectories rather than pooling them with light-duty traffic, the analysis examines behavioral differences that may be obscured in aggregate evaluations. The study also evaluates whether vehicle-category representation and calibration affect fuel-consumption estimates for heavy vehicles. Together, this category-aware evaluation supports the assessment of

behavioral modeling assumptions when microsimulation outputs are used for energy and emissions analysis in mixed traffic environments.

2 Background

2.1 Car Following Models in Microsimulation

Car-following models specify how a following vehicle adjusts its speed in response to the leader. A wide range of formulations has been proposed, from early models by Reuschel and Pipes to modern parametric and data-driven approaches [11]–[13]. SUMO implements several widely used car-following formulations, including the Krauss model, the Intelligent Driver Model (IDM), the Enhanced Intelligent Driver Model (EIDM), and the Wiedemann 99 (W99) model. The present study focuses on the Intelligent Driver Model (IDM) for detailed trajectory-level evaluation though analysis was done for each of the mentioned models with results provided in Appendix.

Intelligent Driver Model (IDM) The IDM [14] describes acceleration as a continuous function of speed, spacing, and relative speed:

$$\dot{v}_f = a\left[1 - \left(\frac{v_f}{v_0}\right)^{\delta} - \left(\frac{s^*(v_f, \Delta v)}{s}\right)^2\right], \tag{1}$$

where the desired gap is

$$s^*(v_f, \Delta v) = s_0 + \tau v_f + \frac{v_f \Delta v}{2\sqrt{ab}}. \tag{2}$$

In these equations, v_f is the follower speed, v_0 is the desired speed, Δv is the relative speed between the follower and leader, s is the current spacing, s^* is the desired spacing, a is the maximum acceleration parameter, b is the comfortable deceleration parameter, s_0 is the minimum gap, τ is the desired time headway, and δ is the acceleration exponent. These parameters have direct behavioral interpretations, which has contributed to the model's widespread use.

2.2 Source Data Collection

This section summarizes the CF-model calibration methodology presented at the SUMO User Conference 2024 [7] and describes the dataset used in this study. The methodology builds on fused roadside radar trajectories that provide lane-aligned measurements of leader and follower motion at high temporal resolution. These trajectories are used to compute car-following metrics and to assign vehicles to length-based categories. Measured leader motion is replayed in SUMO to support simulation-based analysis of follower behavior.

The Intelligent Driver Model (IDM) is evaluated using both default and calibrated parameter sets. Performance is quantified using trajectory-level error metrics in spacing, velocity, and acceleration. Fuel consumption estimations from PHEMlight are applied within SUMO simulations. Together, these steps define a consistent workflow for relating vehicle category, behavioral assumptions, and calibration to simulated trajectories and fuel-consumption outcomes.

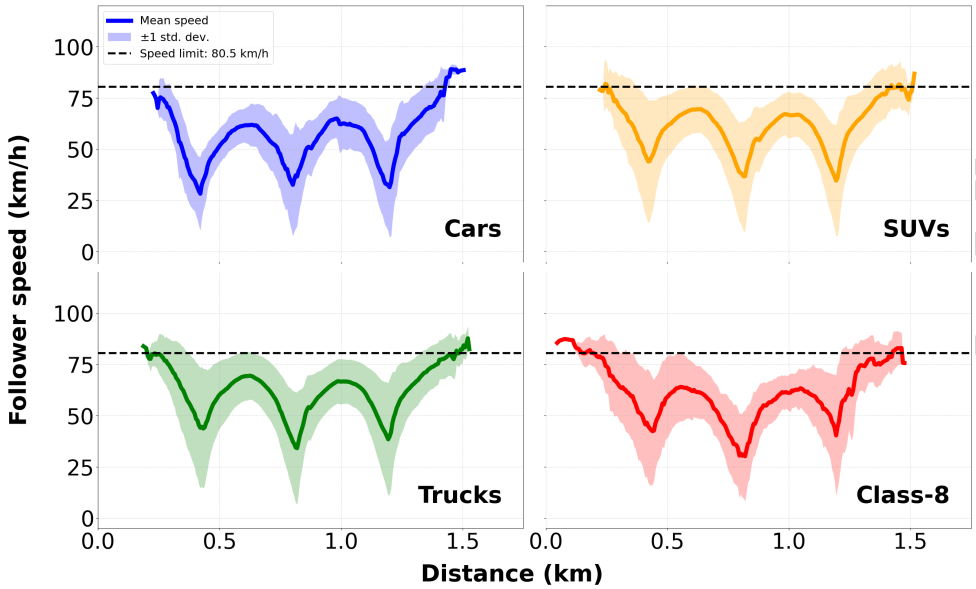

Figure 1. *Radar-derived follower speed profiles shown as longitudinal speed (km/h) versus cumulative distance (km). Panels correspond to Cars (top left), SUVs (top right), Trucks (bottom left), and Class-8 vehicles (bottom right). Solid lines represent category mean profiles, shaded regions represent* ± 1 *standard deviation, and the dashed horizontal line represents the 80.5 km/h corridor speed limit.*

2.2.1 Radar Data and Leader-Follower Pair Identification

This study uses a fused roadside radar trajectory dataset collected along a four-lane divided arterial corridor in Tuscaloosa, Alabama. The dataset was produced using the multi-sensor framework described in [7], [15], resulting in a dataset of continuous lane-aligned trajectories along the corridor. Each trajectory record includes the longitudinal position in the Frenet frame, the speed signal, a radar-based estimate of vehicle length, lane assignment and lane index, and, when available, the identifier of the vehicle directly ahead. These fields support the identification of leader–follower relationships, the computation of spacing and headway, and the assignment of vehicles to length-based categories. The fused and resampled trajectories form the common data source for the car-following analysis, the SUMO simulations, and the fuel-consumption analysis across Cars, SUVs, Trucks, and Class-8 vehicles.

Figure 1 summarizes the radar-derived follower speed profiles as a function of cumulative distance by vehicle category. The profiles show repeated speed reductions along the corridor, consistent with operation through the signalized intersections. The mean speed does not generally fall to zero, indicating that not all vehicles stop at each signal. Mean speeds are higher near the beginning and end of the plotted corridor than in the middle portion, which is consistent with the radar domain not extending to the upstream and downstream signals outside the captured segment.

2.2.2 Vehicle Length Extraction and Classification

Differing from our prior works on trajectory calibration, the radar-reported vehicle length is used to classify vehicles into the most common types found on the road in the local region. The reported radar length varies along a trajectory due to changes in viewing angle and partial detections. To obtain a stable per-vehicle estimate, a single representative length is defined as the maximum reported value over the trajectory,

Table 1. *Gaussian length distribution parameters used for radar-based vehicle categorization.*

Category	μ (m)	σ (m)	Lower Bound (m)	Upper Bound (m)
Car	4.78	0.42	4.06	5.49
SUV	4.97	0.38	4.32	5.61
Truck	5.72	0.67	4.57	6.86
Class-8	15.75	2.48	11.50	20.00

$$L_{\max}(i) = \max_t L_s(i,t). \tag{3}$$

Here, $L_{\max}(i)$ is the representative length assigned to vehicle i, $L_s(i,t)$ is the radar-reported length of vehicle i at time t, and $\max_t$ denotes the maximum value over all observations in the trajectory. Using the maximum reduces sensitivity to systematic underestimation that occurs when only a portion of a vehicle is captured within the sensor field of view [15]. However, this approach can be sensitive to occasional overestimation when detections are affected by tracking errors or closely spaced vehicles. To reduce this effect, the classification procedure does not assign vehicles to a category when their representative length falls outside the published category length bounds. This scalar length measure serves as the primary input for vehicle category assignment.

Vehicles are assigned to four classes using the Gaussian length-based procedure where each radar-observed vehicle is assigned to one of four categories, Car, SUV, Truck, or Class-8, based on the statistical likelihood of its representative length under category-specific distributions.

For each category, a normal distribution is defined using published vehicle length ranges. Length ranges for Cars, SUVs, and light-duty Trucks are taken from publicly reported vehicle dimension statistics [16]. The Class-8 length range is taken from published heavy-vehicle dimensions [17]. The Gaussian parameters are computed directly from the reported lower and upper bounds, with μ defined as the midpoint of the range and σ calculated from the range width under the assumption of a uniform distribution within the reported limits for each category. The resulting values are summarized in Table 1. Lower and upper bounds restrict assignments to the published limits.

For each vehicle, the representative length $L_{\max}(i)$ is evaluated under the four category-specific distributions. If the length falls outside the admissible range for a given category, the likelihood for that category is set to zero. Among the remaining categories, the vehicle is assigned to the category with the highest likelihood. This probabilistic formulation accounts for variability in radar-based length estimates caused by viewing geometry and partial detections.

The fused radar dataset contains 73,084 vehicle trajectories collected over the 24-hour study period [7]. After applying the leader–follower identification procedure 2,351 valid leader–follower pairs remain. In this context, valid pairs are retained pairs with an identified leader, sufficient temporal overlap between the leader and follower trajectories, consistent lane assignment, and physically meaningful leader–follower ordering. Invalid cases include trajectories without an assigned leader, insufficient shared observation time, lane mismatches, or inconsistent longitudinal ordering. The Gaussian length classification is applied to the follower vehicles within these pairs. Of the 2,351 follower vehicles in valid pairs, 1,815 fall within the defined length bounds and are categorized as 250 Cars, 607 SUVs, 878 Trucks, and 80 Class-8 vehicles.

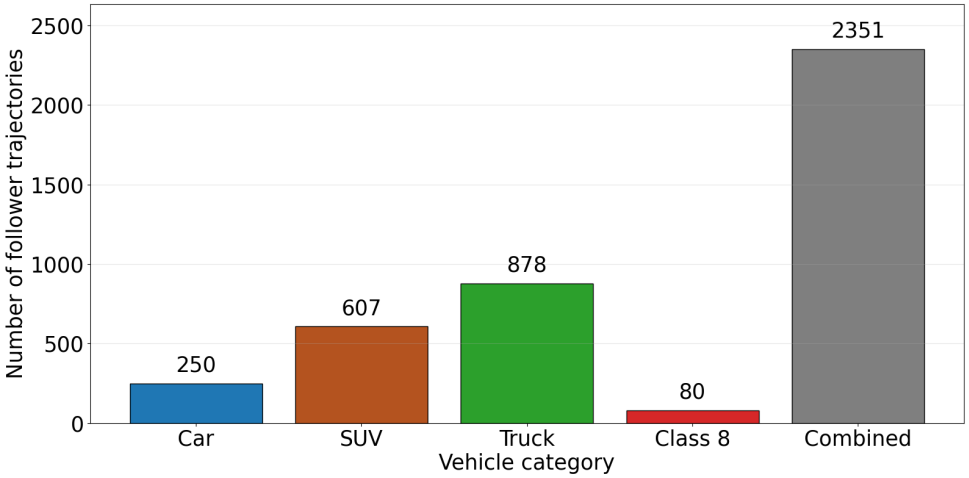

Figure 2. *Number of radar-derived follower trajectories assigned to each vehicle category.*

Figure 2 presents the distribution of classified follower trajectories. These vehicle class labels are retained throughout the study so that car-following behavior and fuel-consumption analyses are reported consistently by vehicle category.

2.2.3 Car-Following Metrics

The fused radar trajectories provide lane-aligned measurements of leader and follower motion at a uniform sampling interval of 0.1 s. For each observation, the dataset includes the longitudinal position in the Frenet frame, the follower velocity, a radar-based estimate of vehicle length, and an identifier for the vehicle directly ahead when a leader is present. These quantities are sufficient to construct kinematic measures that describe longitudinal car-following behavior.

Spacing is defined as the bumper-to-bumper distance between the leader and the follower,

$$g(t) = s_{\text{lead}}(t) - s_{\text{follow}}(t) - L_{\text{lead}}(t), \tag{4}$$

where $s_{\text{lead}}(t)$ and $s_{\text{follow}}(t)$ denote the Frenet-aligned longitudinal positions of the leader and follower, respectively, and $L_{\text{lead}}(t)$ is the radar-reported length of the leader vehicle.

Time headway is computed as

$$\tau(t) = \frac{s_{\text{lead}}(t) - s_{\text{follow}}(t)}{v_{\text{follow}}(t)}, \tag{5}$$

which represents the instantaneous temporal separation between vehicles.

Follower acceleration is approximated by differentiating the follower velocity signal with respect to time using the fixed 0.1 s sampling interval. This finite-difference approximation provides a consistent estimate of longitudinal acceleration across all trajectories.

After spacing, headway, speed, and acceleration are computed, observations that are not physically meaningful are excluded from further analysis. These include instances of negative spacing and headway values inflated by follower velocities approaching zero. While not prevalent in the dataset, this filtering step ensures that subsequent analyses reflect realistic vehicle motion.

For each radar-identified follower trajectory, summary measures are extracted over the overlapping leader-follower interval. These include the minimum spacing, $s_{0,\min}$, and minimum time headway, $\tau_{\min}$, observed during the interaction, along with the 95th percentile positive acceleration, a_{95}, and the 95th percentile deceleration magnitude, b_{95}. The 95th percentile acceleration and deceleration values are used to reduce the influence of isolated acceleration or deceleration spikes while still representing stronger longitudinal responses within each trajectory. Near-zero acceleration and deceleration observations were retained in the trajectory data when these summary measures were computed. Differentiating from prior work, the resulting distributions characterize longitudinal behavior across the four vehicle categories, rather than as a combined dataset, and form the basis for the comparative analyses presented in the following sections.

Figure 3 summarizes the empirical distributions of the computed car-following metrics for radar-identified follower vehicles. Distributions are shown by vehicle category and for the *Combined* group. The Combined group represents the full set of radar-identified follower trajectories prior to vehicle categorization and reflects the overall longitudinal behavior observed in the dataset.

The light-duty categories, Cars, SUVs, and Trucks, exhibit similar distributions in a_{95} and b_{95}. Most trajectory-level values remain below approximately 3–4 m/s^2, indicating moderate longitudinal responses under the signalized corridor conditions. Class-8 vehicles show a shift in time headway toward larger values, with upper percentiles exceeding 5 s. This indicates longer following gaps relative to light-duty traffic. Minimum spacing distributions are broadly comparable across categories, although Class-8 vehicles tend to operate at slightly larger typical gaps.

The a_{95} and b_{95} distributions for Class-8 vehicles overlap with those of the light-duty categories, reflecting similar ranges of observed longitudinal response. A slight shift toward larger values is visible for Class-8 vehicles, but differences between categories are more evident in following behavior. Class-8 vehicles exhibit larger time headway values, with a median of 2.65 s compared to approximately 2.0 s for Cars, SUVs, and Trucks. Minimum spacing values are also larger for Class-8 vehicles, with a median of 7.22 m compared to approximately 5–6 m for the light-duty categories. These observed differences in headway and spacing indicate that Class-8 vehicles maintain larger longitudinal separation in the measured radar trajectories.

2.2.4 Fuel Estimation Methods

Fuel consumption is estimated using the PHEMlight emissions model as implemented within SUMO. Measured radar leader trajectories are replayed in SUMO via TraCI, while follower vehicles are simulated using the selected car-following model and parameter set. Fuel consumption is computed internally by SUMO using PHEMlight, which provides fuel-rate estimates based on the simulated vehicle dynamics and the assigned vehicle class [18], [19].

Each simulated follower is assigned an emissions class consistent with its radar-based vehicle category. Passenger cars use a gasoline passenger-car class, while SUVs and light-duty trucks use a light commercial vehicle class. Class-8 vehicles are assigned a heavy-duty diesel tractor–trailer class, following the PHEMlight definitions available within SUMO [19]. Only follower vehicles are retained for analysis, since the objective is to evaluate how differences in simulated following behavior influence fuel consumption.

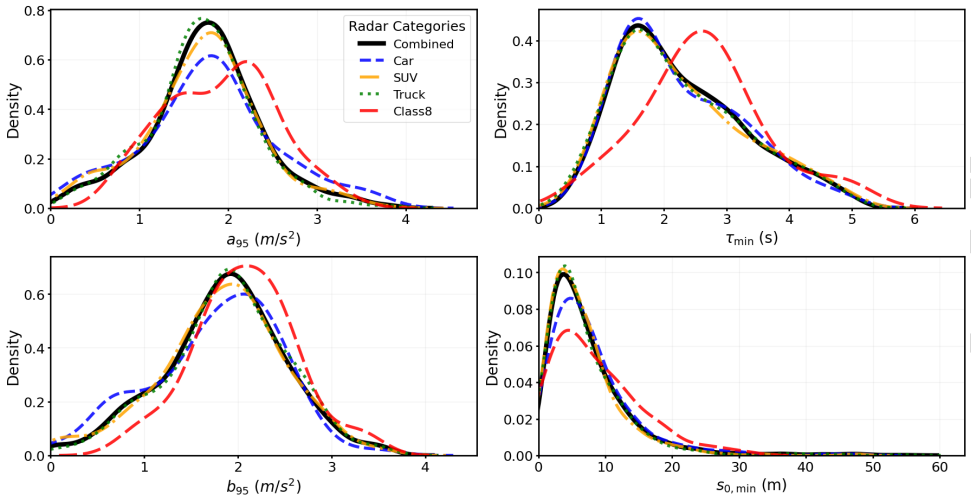

Figure 3. *Kernel density estimates of car–following metrics computed from the fused radar trajectories. The four panels show the distributions of 95th percentile positive acceleration, a_{95}, minimum time headway, τ_{min}, 95th percentile deceleration magnitude, b_{95}, and minimum spacing, $s_{0,\text{min}}$, for all vehicles and for each radar-based category.*

SUMO provides instantaneous fuel-rate outputs for each simulated vehicle through the PHEMlight emissions interface. In the exported emissions files, fuel rate is reported in milligrams per second, mg/s. For each follower trajectory, fuel rate is integrated over time using the simulation timestep to obtain total fuel mass. The resulting fuel mass is converted to liters using a category-specific fuel density. Trajectory-level fuel consumption is reported in L/100 km by normalizing total fuel volume by the distance traveled, allowing trajectories with different travel distances to be compared on a common basis. Distance is computed from the simulated longitudinal position over the trajectory.

2.3 SUMO Simulation Setup

The SUMO experiments build on the leader-follower evaluation framework presented in [7] and use the SUMO microsimulation platform for trajectory replay and follower simulation [19] to support vehicle-category analysis and the fuel estimation methods described in Section 2.2.4. All simulations are conducted on a single straight link of length 1.5 km, which is sufficient to accommodate the full extent of the radar-derived trajectories. The link speed limit is set to 22.35 m/s to match the posted limit on the study corridor.

For each radar-identified leader–follower pair, the measured leader trajectory is imposed through TraCI. At every simulation step, the leader's longitudinal position and speed are set to the corresponding radar values. The follower vehicle is simulated using one of the car-following models introduced earlier in the Methods section. SUMO records the follower speed, position, and spacing relative to the radar-based leader, enabling direct trajectory-level comparison with the observed follower behavior.

Vehicle categories obtained in Section 2.2.2 are incorporated directly into the simulation setup. Each follower is assigned a SUMO `vClass` consistent with its radar-based category, ensuring that the associated PHEMlight emission class aligns with the representative vehicle class used for fuel estimation. This preserves consistency between vehicle categorization, simulated dynamics, and fuel estimation.

To support the fuel analysis, each simulation produces an emissions output file containing PHEMlight fuel-rate estimates aligned with the simulated trajectories. Other simulation settings follow the configuration reported in [7], including ballistic integration and a 0.1 s simulation step, consistent with the resampled radar trajectories. Emission outputs are recorded at the same temporal resolution.

The Intelligent Driver Model (IDM) is evaluated. For each vehicle category, simulations are conducted using the default SUMO parameter set and a calibrated parameter set obtained using the $\mathrm{NRMSE}_{s,v,a}$ objective described in [7]. This setup yields category-consistent simulated trajectories and PHEMlight fuel-rate outputs, providing a common basis for evaluating how car-following behavior and calibration state influence fuel-consumption estimates across vehicle classes.

3 Results

This section reports car following and fuel consumption results from the radar-based leader-follower simulations and radar-based estimates described in Section 2.2. Results are reported by vehicle category. The vehicle categories are Car, SUV, Truck, and Class-8. Results compare the default IDM parameter set with parameters calibrated using the $\mathrm{NRMSE}_{s,v,a}$ objective, which reduces the combined normalized error in follower spacing, velocity, and acceleration.

Results first summarizes how calibrated parameter values vary by vehicle category. Then an evaluation of trajectory level reproduction error in spacing, velocity, and acceleration is presented followed by a focused Class-8 analysis to examine sensitivity to representing heavy trucks with passenger car assumptions. Finally, fuel consumption results across categories using PHEMlight within SUMO highlight potential impact of the driver behavior calibration and classification determination.

3.1 Car–Following Behavior by Category

This subsection examines how calibrated car-following parameters vary across vehicle categories, with emphasis on differences between Class-8 vehicles and light-duty traffic. Results are presented by vehicle category to identify category-dependent trends within the IDM formulation.

In addition to the category-specific calibrations, an *uncategorized* or *Combined calibration* is included in which all trajectories are pooled prior to vehicle categorization and simulated in SUMO using passenger-car vehicle definitions. This case primarily reflects light-duty driving behavior and is used as a baseline reference for interpreting category-specific deviations.

Figure 4 presents the calibrated parameter distributions for IDM. That is, the distribution of best fit parameters across all vehicles in each category that best minimized the NRMSE for spacing, speed, and acceleration. By combining the best fit parameters in this way, the distribution of driver behavior is captured rather than simply the mean value.

For the acceleration parameter, Cars, SUVs, and Trucks closely track the combined calibration, which has a median value of 2.601 $\mathrm{m/s^2}$ while Class-8 vehicles exhibit lower

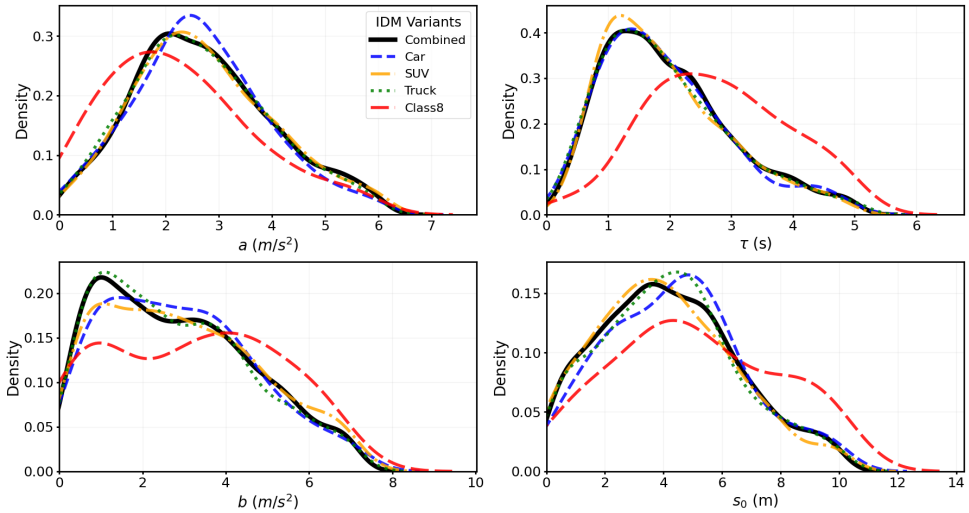

Figure 4. *Distributions of calibrated IDM parameters for each vehicle category compared with the combined calibration. Thick black curves show the combined (uncategorized) calibration, while colored dashed curves show the category-specific results.*

acceleration values, with a median of 2.052 m/s^2. Differences between categories are similar for time headway parameter, τ, with combined calibration having a median of 1.781 s, and Cars, SUVs, and Trucks having very similar values. Again, in contrast, the Class-8 distribution shifts toward larger headways, with a median of 2.693 s.

For deceleration and minimum gap parameters, slight differences between all classifications emerge though Class-8 is still the most distinct among the four. In fact, the Class-8 behavior seems to show bimodal distributions indicating distinct driving conditions. Further analysis of raw data would be required, but it is not hard to imagine a harder deceleration event leading to a shorter minimum gap. This is not necessarily the drivers desired behavior, but a consequence of surrounding traffic.

These trends are largely intuitive based on how a commercial vehicle operator of a large truck would likely have a different and more conservative mindset when following traffic through a signalized corridor. These parameter differences correspond directly to the measured radar trajectory behavior shown in Figure 3. The calibrated IDM acceleration parameter for Class-8 vehicles is lower than that of the light-duty categories, and the calibrated time headway parameter is larger. These differences are consistent with the longer headways and larger spacing values observed in the measured radar trajectories. This agreement indicates that the calibrated IDM parameters capture the primary category-specific trends observed in the measured radar data.

3.2 Calibration Error

The calibrated IDM parameter distributions presented in Section 3.1 are the set of parameters that best match the observed follower behavior. Here, the calibration is evaluated using trajectory-level reproduction error, NRMSE$_{s,v,a}$, in the final calibrated behavior for each vehicle in the category specific dataset. Figure 5 presents trajectory-level RMSE distributions for the default IDM parameter. Note that trajectories flagged as collisions were excluded from this analysis. Only one simulated trajectory was flagged as a collision and excluded from the analysis, occurring in the uncalibrated SUV case.

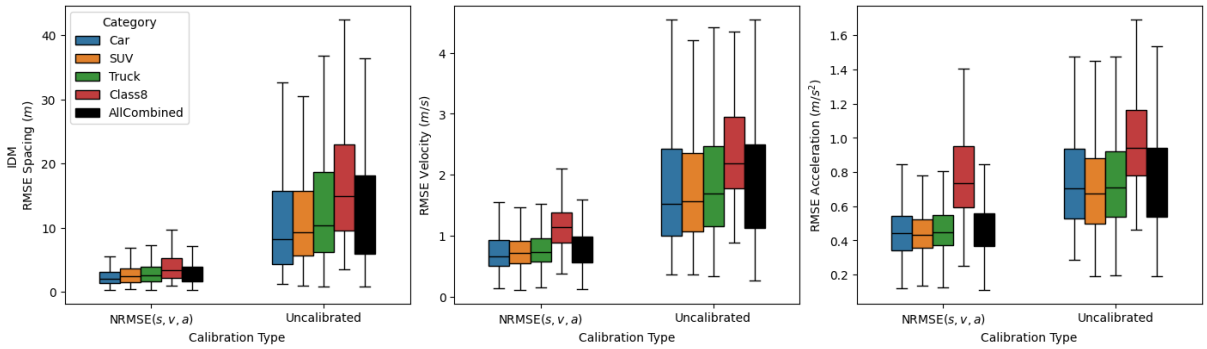

Figure 5. *Distributions of trajectory-level RMSE in spacing, velocity, and acceleration for the default IDM parameter set and the* $\mathrm{NRMSE}_{s,v,a}$ *calibrated IDM simulations, shown by vehicle category. Boxes indicate the interquartile range with the median marked, and whiskers extend to the most extreme values excluding outliers.*

It is clear that across all vehicle categories, calibration reduces the median RMSE in spacing, velocity, and acceleration. The largest reductions occur in spacing error, followed by velocity, while acceleration shows smaller changes. The interquartile ranges are also much narrower after calibration.

For Class-8 vehicles, median spacing RMSE decreases from 14.95 m under the default parameters to 3.40 m after calibration. In the light-duty categories, spacing RMSE decreases from 8.22 m to 2.00 m for Cars, from 9.34 m to 2.41 m for SUVs, and from 10.37 m to 2.53 m for Trucks. The Combined category decreases from 10.22 m to 2.46 m.

Velocity RMSE decreases across categories as well. Focusing on Class-8 vehicles, velocity RMSE decreases from 2.19 m/s to 1.15 m/s. Acceleration RMSE decreases in all categories, although the magnitude of improvement is smaller than for spacing and velocity. For Class-8 vehicles, acceleration RMSE decreases from 0.94 m/s^2 to 0.74 m/s^2.

After calibration, Class-8 vehicles retain slightly higher median RMSE values than Cars, SUVs, and Trucks across spacing, velocity, and acceleration. This could be for a number of reasons, but most likely is due to the challenges in classifying the Class-8 trucks in the radar dataset and then filtering the data effectively. Due to large size of the Trailers, the apparent position reported can change in step fashion as the centroid of the object detected can shift resulting in non-physical apparent position dynamics.

3.3 Class-8 Behavior

Clearly, the Class-8 trucks have different behavior, but it remains to be seen the effect of this on broader simulation. Of course SUMO includes default parameters for heavy trucks with trailers. The results in Section 3.2 evaluated Class-8 trajectories in SUMO using a heavy-duty vehicle-type definition, denoted as *Class-8* in the figures. This subsection examines whether the reproduction of Class-8 following behavior changes when the same radar-observed leader–follower trajectories are simulated using a passenger-car vehicle-type definition denoted as *Class8-PC*. In this comparison, the same observed trajectories are used, while the follower vehicle-type assignment is changed from trailer to passenger car. This could occur in simulations without knowledge of vehicle classification or without vehicle classification distribution knowledge.

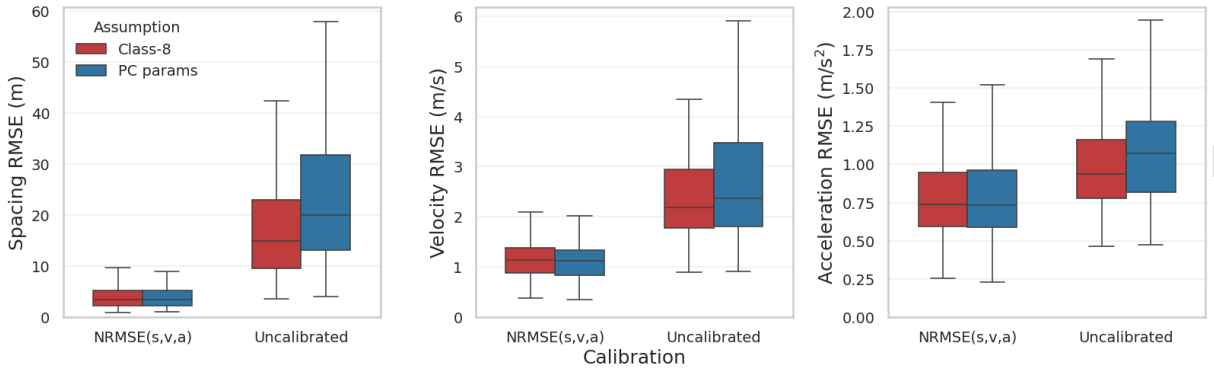

Figure 6. *Distributions of trajectory-level RMSE in spacing, velocity, and acceleration for Class-8 and Class8-PC vehicle representations using the IDM car-following model. Results are shown for uncalibrated simulations and simulations calibrated using* $\text{NRMSE}_{s,v,a}$.

To isolate the effect of the vehicle representation, the same observed trajectories, imposed leader motion, calibration procedure, and simulation configuration are used in both cases. The only difference between the two simulations is the vehicle-type assignment applied to the follower vehicle, including its associated emission class in PHEMlight. Figure 6 compares trajectory-level RMSE in spacing, velocity, and acceleration for Class-8 and Class8-PC simulations under uncalibrated parameters and parameters calibrated using $\text{NRMSE}_{s,v,a}$.

For the uncalibrated simulations, spacing RMSE is higher under the Class8-PC representation. The median spacing RMSE increases from 14.95 m under Class-8 to 19.98 m under Class8-PC. Velocity RMSE differs less between the two representations, with the median increasing from 2.19 m/s to 2.37 m/s. Acceleration RMSE also increases under Class8-PC, from 0.94 m/s^2 to 1.07 m/s^2. This shows that by using the correct vehicle-type assignment, which uses different default CF parameters, there is some improvement to the overall ability to represent the real-world observations. However, after calibration there is really no difference in observed behavior as the default parameters are superseded.

While the RMSE results summarize trajectory-level reproduction error, they do not describe how well the simulated trajectories reflect the distribution of observed Class-8 behavior over the full trajectories. Empirical cumulative distribution functions (ECDFs) are used in lieu of analyzing individual trajectories as shown in Figure 7 for follower velocity, acceleration, and time headway. In an ECDF, the y-axis represents the cumulative fraction of observations at or below each value on the horizontal axis. Results are shown for the Class-8 and Class8-PC representations under uncalibrated parameters and parameters calibrated using $\text{NRMSE}_{s,v,a}$ and compared to the radar measured distributions.

In the uncalibrated/default simulations, differences between the two representations are most apparent in the acceleration and headway distributions with large deviation from the real-world behavior. Specifically, the default parameters have generally too aggressive of an acceleration, do not modulate the acceleration as speed increases and have non-physical peak acceleration behavior due to lack of distributional data in default configuration. Further, the default parameter headway for both passenger and trailer vehicle-types still have much shorter headway than drivers in the test region seem to prefer. After the calibration procedures, the separation between the Class-8 and Class-8-PC cases is reduced across velocity, acceleration, and headway. Calibra-

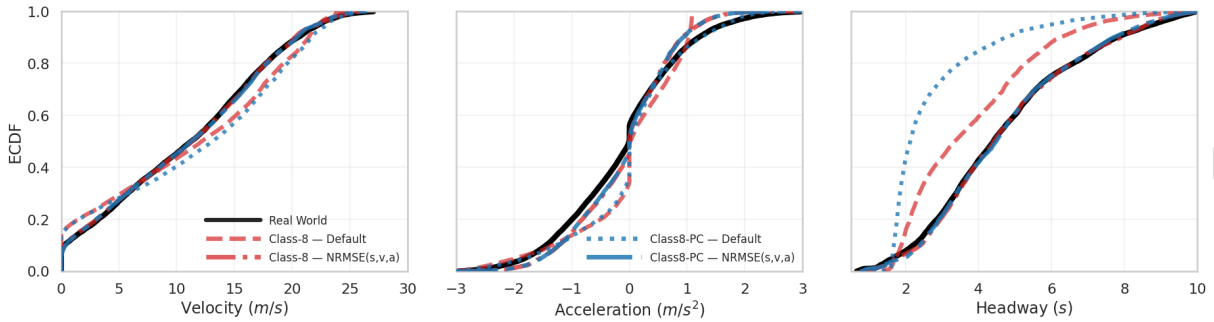

Figure 7. *Empirical cumulative distribution functions (ECDFs) of follower velocity, acceleration, and headway for Class-8 and Class8-PC vehicle representations using the IDM. Results are shown for uncalibrated simulations and simulations calibrated using* NRMSE$_{s,v,a}$.

tion improves distributional alignment and are consistent with the trajectory-level RMSE results. Of course, the regional driving behavior is not guaranteed to capture other areas so before making suggestions to update default parameters it would be desirable to do similar evaluation in other cities and countries.

3.4 Fuel-Consumption Estimates Across Categories

After evaluating the classification-specific driving behavior, the discussion will now shift to focus on the impacts to trajectory-level fuel consumption estimations. PHEMlight-based fuel consumption is obtained from the IDM simulations described in Section 2.3, In all cases, emission classes and vehicle parameters are assigned according to the radar-based vehicle category. Fuel consumption is reported per trajectory by integrating instantaneous fuel rate over time and normalizing by distance traveled to yield L/100 km.

Figure 8 presents trajectory-level PHEMlight fuel-consumption distributions for the Default and NRMSE$_{s,v,a}$ calibrated IDM parameter sets, shown by vehicle category. For each vehicle category, calibration reduces the median fuel consumption. The median decreases by 12% for Cars, 10% for SUVs, 8.5% for Trucks, and 12.7% for Class-8 vehicles.

For Cars, SUVs, and Trucks, the interquartile ranges are similar between the Default and calibrated cases, and the distributions overlap. Class-8 vehicles exhibit a substantially larger spread than the light-duty categories under both parameter sets. These fuel-consumption trends align with the reproduction-error results reported in Section 3.2, where calibration reduced spacing and velocity error across categories.

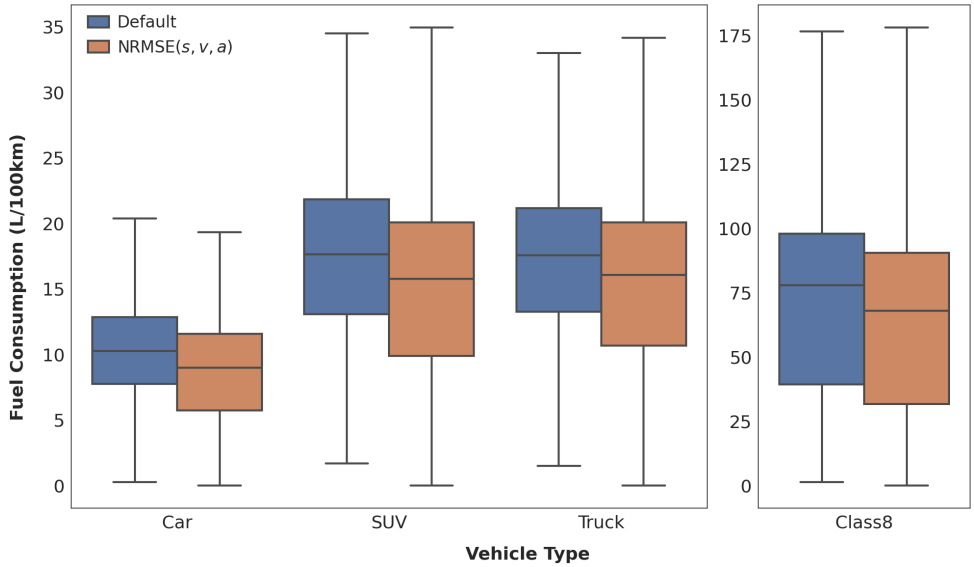

Figure 8. *Trajectory-level PHEMlight fuel-consumption distributions under the Default and* $\text{NRMSE}_{s,v,a}$ *calibrated IDM parameter sets. The left panel shows Cars, SUVs, and Trucks. The right panel shows Class-8 vehicles. Boxes indicate the interquartile range with the median marked, and whiskers extend to the most extreme values excluding outliers.*

4 Summary, Conclusions & Future Work

This work evaluated how well the Intelligent Driver Model (IDM) reproduces observed leader–follower behavior across vehicle categories and how these behavioral differences influence PHEMlight fuel-consumption estimates in SUMO. Using fused roadside radar extracted real-world trajectories from a 1.5 km signalized corridor, measured leader motion was replayed in SUMO via TraCI and follower trajectories were simulated using the IDM car following model. Followers were classified into Cars, SUVs, light-duty Trucks, and Class-8 vehicles using radar-reported length. Model performance was quantified using trajectory-level RMSE in spacing, velocity, and acceleration, and fuel consumption was computed from SUMO emissions outputs using PHEMlight.

Across all categories, calibration reduced trajectory-level RMSE in spacing, velocity, and acceleration. The largest reductions occurred in spacing, while velocity and acceleration showed smaller changes. After calibration, Class-8 trajectories retained higher reproduction error than Cars, SUVs, and light-duty Trucks across all three metrics, indicating that heavy-truck following behavior was less well captured within the IDM framework under the study conditions or that the radar obtained trajectories may be of lower quality.

Regardless, this focused Class-8 representation analysis compared simulations using default and calibrated IDM models when treating Class-8 trucks as both `vClass` *passenger* and *trailer*. A situation that would be common if models are not aware of the vehicle classification. Under the default parameter sets, the Class8-PC case (i.e. treat a Class-8 vehicle as a passenger car) exhibited high spacing and acceleration error.

Fuel-consumption results varied by calibration state and vehicle category as may be expected with PHEMlight fuel-consumption medians decreasing after calibration for each category, with the largest absolute reduction observed for Class-8 vehicles. These

changes occur alongside the reductions in spacing and velocity error reported in Section 3.2, indicating that trajectory-level calibration can materially affect energy estimates derived from microsimulation.

Future work will expand the set of usable Class-8 leader–follower pairs and further evaluate heavy-vehicle representation within the trajectory-replay framework. The current dataset contains fewer classified Class-8 pairs than the light-duty categories after filtering and quality checks, which limits coverage of operating conditions. Increasing the Class-8 sample will support more robust calibration and evaluation across a wider range of speeds and interactions. Additional work will also refine heavy-vehicle trajectory processing and classification to reduce uncertainty associated with tractor–trailer detections and to strengthen category-specific interpretation of microsimulation outputs used for energy and emissions analysis.

CRediT authorship contribution statement

Mahdi Al Abdraboh: Conceptualization, Methodology, Software, Formal Analysis, Visualization, Writing - original draft, Writing - review & editing. **Joshua Bittle:** Conceptualization, Methodology, Resources, Writing - review & editing, Supervision, Project administration, Funding acquisition.

Acknowledgments and Declarations

This material is based upon work supported by the U.S. Department of Energy's Office of Energy Efficiency and Renewable Energy (EERE) under the the Vehicle Technologies Office (VTO) and through Energy Efficient Mobility Systems (EEMS) program award number DE-EE0009210. The views expressed herein do not necessarily represent the views of the U.S. Department of Energy or the United States Government. This work was also supported by The University of Alabama's Center for Advanced Vehicle Technology (CAVT). The author gratefully acknowledges scholarship support from the Saudi Arabian Cultural Mission (SACM).

The authors have no conflicts of interests to declare that are relevant to the content of this article. Currently data provided by request to corresponding author, though future plans include making this data and more from the dataset publicly available online.

References

[1] Z. Cui, X. Wang, Y. Ci, C. Yang, and J. Yao, "Modeling and analysis of car-following models incorporating multiple lead vehicles and acceleration information in heterogeneous traffic flow," *Physica A: Statistical Mechanics and its Applications*, vol. 630, p. 129 259, 2023. DOI: 10.1016/j.physa.2023.129259.

[2] S. Zhou, J. Tian, Y.-E. Ge, S. Yu, and R. Jiang, "Experimental features of emissions and fuel consumption in a car-following platoon," *Transportation Research Part D: Transport and Environment*, vol. 121, p. 103 823, 2023. DOI: 10.1016/j.trd.2023.103823.

[3] K. Biszko, J. Oskarbski, and K. Żarski, "Impact of different car-following models on estimating safety and emissions on signal-controlled intersections using microscopic simulations," *Archives of Transport*, vol. 72, no. 4, pp. 43–73, 2024. DOI: 10.61089/aot2024.eb2hfe27.

[4] X. Yao, Q. Yan, Z. Sun, S. C. Calvert, and S. P. Hoogendoorn, "Investigation on car-following heterogeneity and its impacts on traffic safety and sustainability," *Transportmetrica A: Transport Science*, pp. 1–25, 2024. DOI: 10.1080/23249935.2024.2407077.

[5] M. Schrader, M. Al Abdraboh, and J. Bittle, "Comparing measured driver behavior distributions to results from car-following models using sumo and real-world vehicle trajectories from radar: Sumo default vs. radar-measured cf model parameters," in *SUMO Conference Proceedings*, vol. 4, 2023, pp. 41–54. DOI: 10.52825/scp.v4i.214.

[6] D. K. Hale, A. Ghiasi, F. Khalighi, D. Zhao, X. (Li, and R. M. James, "Vehicle trajectory-based calibration procedure for microsimulation," *Transportation Research Record*, vol. 2677, no. 1, pp. 1764–1781, 2023. DOI: 10.1177/03611981221124597.

[7] M. Schrader, A. Karnik, A. Hainen, and J. Bittle, "Calibrating car-following models using sumo-in-the-loop and vehicle trajectories from roadside radar: Calibrating cf model parameters," in *SUMO Conference Proceedings*, vol. 5, 2024, pp. 209–233. DOI: 10.52825/scp.v5i.1127.

[8] N. Kang, C. Qian, Y. Zhou, and W. Luo, "Operational evaluation of mixed flow on highways considering trucks and autonomous vehicles based on an improved car-following decision framework," *Sustainability*, vol. 17, no. 14, p. 6450, 2025. DOI: 10.3390/su17146450.

[9] A. Boggio-Marzet, A. Monzon, A. M. Rodriguez-Alloza, and Y. Wang, "Combined influence of traffic conditions, driving behavior, and type of road on fuel consumption. real driving data from madrid area," *International journal of sustainable transportation*, vol. 16, no. 4, pp. 301–313, 2022. DOI: 10.1080/15568318.2020.1871128.

[10] J. Guo, H. Guo, Z.-S. Chen, Z. Fan, and W.-L. Shang, "Spatiotemporal analysis of co_2 emissions from heavy-duty trucks in belt and road port transportation using gps trajectory data," *Resources, Conservation and Recycling*, vol. 223, p. 108 540, 2025. DOI: 10.1016/j.resconrec.2025.108540.

[11] A. Reuschel, "Fahrzeugbewegungen in der kolonne," *Osterreichisches Ingenieur Archiv*, vol. 4, pp. 193–215, 1950.

[12] L. A. Pipes, "An operational analysis of traffic dynamics," *Journal of applied physics*, vol. 24, no. 3, pp. 274–281, 1953. DOI: 10.1063/1.1721265.

[13] Y. Zhang, X. Chen, J. Wang, Z. Zheng, and K. Wu, "A generative car-following model conditioned on driving styles," *Transportation research part C: emerging technologies*, vol. 145, p. 103 926, 2022. DOI: 10.1016/j.trc.2022.103926.

[14] M. Treiber, A. Hennecke, and D. Helbing, "Congested traffic states in empirical observations and microscopic simulations," *Physical review E*, vol. 62, no. 2, p. 1805, 2000. DOI: 10.1103/PhysRevE.62.1805.

[15] M. Schrader, A. Hainen, and J. Bittle, "Extracting vehicle trajectories from partially overlapping roadside radar," *Sensors*, vol. 24, no. 14, p. 4640, 2024. DOI: 10.3390/s24144640.

[16] Extra Space Storage, *Average car dimensions: A guide to length, width, & height*, Accessed: 2025-04-28, Mar. 2025. [Online]. Available: https://www.extraspace.com/blog/self-storage/average-car-dimensions/.

[17] R. D. Ervin, R. Nisonger, C. MacAdam, P. Fancher, *et al.*, "Influence of size and weight variables on the stability and control properties of heavy trucks," United States. Department of Transportation. Federal Highway Administration, Tech. Rep., 1986.

[18] Graz University of Technology (TU Graz), *PHEMlight: Passenger Car and Heavy Duty Emission Model (Light Version)*, https://www.itna.tugraz.at/en/research/areas/em/simulation/phemlight.html, Licensed emission and fuel consumption model developed in cooperation with FVTmbH, 2024.

[19] D. I. of Transportation Systems, *PHEMlight Emission Model in SUMO*, https://sumo.dlr.de/docs/Models/Emissions/PHEMlight.html, 2024.

Appendix: Calibrated CF-Model Parameters

The results and analysis in the main document focused on the impacts of the vehicle type classification on the trajectory level reproduction and fuel consumption estimations. Similar trends were observed for the other CF models studied so their detailed analysis was not included. For completeness, the following tables presents the calibrated parameter sets for IDM, EIDM, Krauss and W99, for each vehicle type in similar format to those shared previously [7]. The tables present the calibrated mean (μ) values along with description of the distributions as standard deviation (σ), and the 10th, 50th, and 90th ($P_{10-90th}$) percentiles. The lower and upper bounds of the optimization constraints are also shown for reference. Certain parameters were further constrained to be multiples of the simulation step size, such as actionStepLength.

The SUMO default values for the `passenger` car class or `trailer` class are also provided for reference, with the value being given as the μ. These distributions can be used to generate vehicle distribution files that capture the diverse driver behavior and avoid having each vehicle use the same CF model parameters.

Table 2. *Calibrated results of the IDM CF-model with default parameters for `vClass` passenger and trailer included. LB stands for the lower-bound on optimization and UB the upper bound. All parameters are in the naming convention and units presented in the SUMO documentation.*

Parameter	Calibration LB	Calibration UB	Cal. Target	Calibrated Parameters μ	σ	$P_{10\%}$	$P_{50\%}$	$P_{95\%}$
accel	0.1	6.0	Default Passenger	2.60	-	-	-	-
			Cars	2.66	1.24	1.10	2.55	4.97
			SUVs	2.74	1.32	1.16	2.61	5.16
			Trucks	2.68	1.30	1.04	2.55	5.11
			Default Trailer	1.00	-	-	-	-
			Class-8	2.26	1.38	0.57	2.05	5.01
actionStepLength [a]	0.1	1.0	Default Passenger	0.10	-	-	-	-
			Cars	0.32	0.25	0.10	0.20	0.90
			SUVs	0.35	0.25	0.10	0.30	0.90
			Trucks	0.35	0.26	0.10	0.30	0.90
			Default Trailer	0.10	-	-	-	-
			Class-8	0.45	0.31	0.10	0.40	0.97
decel	0.1	7.0	Default Passenger	4.50	-	-	-	-
			Cars	2.88	1.75	0.72	2.68	6.09
			SUVs	2.96	1.86	0.63	2.77	6.46
			Trucks	2.77	1.78	0.65	2.47	6.08
			Default Trailer	4.00	-	-	-	-
			Class-8	3.19	2.02	0.40	3.13	6.41
delta	1.0	10.0	Default Passenger	4.00	-	-	-	-
			Cars	4.73	2.34	1.39	4.89	8.67
			SUVs	4.81	2.37	1.56	4.82	8.81
			Trucks	4.67	2.34	1.58	4.50	9.01
			Default Trailer	4.00	-	-	-	-
			Class-8	5.21	2.59	1.65	4.84	9.61
minGap	0.1	10.0	Default Passenger	2.50	-	-	-	-
			Cars	4.40	2.34	1.41	4.44	8.75
			SUVs	4.05	2.34	1.02	3.85	8.14
			Trucks	4.22	2.34	1.07	4.14	8.64
			Default Trailer	2.50	-	-	-	-
			Class-8	5.11	2.79	1.29	4.68	9.78
speedFactor	0.8	1.8	Default Passenger	1.00	-	-	-	-
			Cars	1.19	0.27	0.83	1.17	1.68
			SUVs	1.19	0.27	0.84	1.18	1.68
			Trucks	1.18	0.28	0.81	1.16	1.69
			Default Trailer	1.00	-	-	-	-
			Class-8	1.21	0.27	0.89	1.17	1.62
stepping [a]	0.1	1.0	Default Passenger	0.25	-	-	-	-
			Cars	0.54	0.22	0.24	0.56	0.92
			SUVs	0.55	0.22	0.25	0.53	0.95
			Trucks	0.54	0.24	0.21	0.53	0.94
			Default Trailer	0.25	-	-	-	-
			Class-8	0.54	0.24	0.21	0.57	0.93
tau	0.1	5.0	Default Passenger	1.00	-	-	-	-
			Cars	1.94	1.03	0.83	1.74	4.14
			SUVs	1.93	1.01	0.82	1.73	3.88
			Trucks	1.94	1.06	0.74	1.76	4.03
			Default Trailer	1.00	-	-	-	-
			Class-8	2.76	1.13	1.47	2.69	4.67

[a] Constrained in optimization to a multiple of the simulation step size

Table 3. *Calibrated results of the EIDM CF-model with default parameters for `vClass` passenger and trailer included. LB stands for the lower-bound on optimization and UB the upper bound. All parameters are in the naming convention and units presented in the SUMO documentation.*

Parameter	Calibration LB	Calibration UB	Cal. Target	Calibrated Parameters μ	σ	$P_{10\%}$	$P_{50\%}$	$P_{95\%}$
accel	0.1	6.0	Default Passenger	2.60	-	-	-	-
			Cars	2.53	1.30	0.96	2.37	4.90
			SUVs	2.46	1.26	0.88	2.34	4.68
			Trucks	2.45	1.25	0.92	2.30	4.79
			Default Trailer	1.00	-	-	-	-
			Class-8	2.15	1.39	0.60	1.97	4.69
actionStepLength [a]	0.1	1.0	Default Passenger	0.10	-	-	-	-
			Cars	0.21	0.18	0.10	0.10	0.60
			SUVs	0.22	0.19	0.10	0.10	0.70
			Trucks	0.22	0.19	0.10	0.10	0.70
			Default Trailer	0.10	-	-	-	-
			Class-8	0.34	0.25	0.10	0.30	0.90
decel	0.1	7.0	Default Passenger	4.50	-	-	-	-
			Cars	2.68	1.63	0.55	2.68	5.72
			SUVs	2.48	1.79	0.29	2.17	5.99
			Trucks	2.49	1.81	0.38	2.22	6.08
			Default Trailer	4.00	-	-	-	-
			Class-8	2.48	2.01	0.14	2.01	6.29
delta	1.0	10.0	Default Passenger	4.00	-	-	-	-
			Cars	5.17	2.29	1.72	5.27	9.26
			SUVs	5.28	2.31	2.08	5.30	9.29
			Trucks	5.15	2.34	1.81	5.15	9.27
			Default Trailer	4.00	-	-	-	-
			Class-8	5.27	2.24	2.31	5.04	9.07
minGap	0.1	10.0	Default Passenger	2.50	-	-	-	-
			Cars	4.31	2.40	1.42	4.07	8.84
			SUVs	4.13	2.28	1.14	3.99	8.34
			Trucks	4.21	2.44	0.94	4.11	8.71
			Default Trailer	2.50	-	-	-	-
			Class-8	5.12	2.55	1.62	4.89	9.51
speedFactor	0.8	1.8	Default Passenger	1.00	-	-	-	-
			Cars	1.23	0.28	0.83	1.24	1.72
			SUVs	1.19	0.28	0.81	1.19	1.68
			Trucks	1.19	0.29	0.80	1.18	1.68
			Default Trailer	1.00	-	-	-	-
			Class-8	1.21	0.30	0.81	1.17	1.75
stepping [a]	0.1	1.0	Default Passenger	0.25	-	-	-	-
			Cars	0.53	0.22	0.22	0.54	0.89
			SUVs	0.53	0.23	0.21	0.53	0.92
			Trucks	0.56	0.23	0.24	0.55	0.95
			Default Trailer	0.25	-	-	-	-
			Class-8	0.56	0.25	0.22	0.55	0.99
tau	0.1	5.0	Default Passenger	1.00	-	-	-	-
			Cars	2.15	1.07	0.93	2.01	4.14
			SUVs	2.18	1.13	0.83	2.01	4.19
			Trucks	2.20	1.13	0.85	2.10	4.38
			Default Trailer	1.00	-	-	-	-
			Class-8	3.02	1.31	1.30	2.91	4.97

[a] Constrained in optimization to a multiple of the simulation step size

Table 4. *Calibrated results of the Krauss CF-model with default parameters for `vClass` passenger and trailer included. LB stands for the lower-bound on optimization and UB the upper bound. All parameters are in the naming convention and units presented in the SUMO documentation.*

Parameter	Calibration LB	Calibration UB	Cal. Target	Calibrated Parameters μ	σ	$P_{10\%}$	$P_{50\%}$	$P_{95\%}$
accel	0.1	7.0	Default Passenger	2.60	-	-	-	-
			Cars	2.62	1.35	1.10	2.47	5.08
			SUVs	2.53	1.31	1.05	2.34	5.03
			Trucks	2.64	1.40	1.08	2.45	5.47
			Default Trailer	1.00	-	-	-	-
			Class-8	2.83	1.71	0.90	2.61	6.44
actionStepLength [a]	0.1	1.0	Default Passenger	0.10	-	-	-	-
			Cars	0.37	0.27	0.10	0.30	0.90
			SUVs	0.38	0.27	0.10	0.30	0.90
			Trucks	0.40	0.28	0.10	0.30	0.90
			Default Trailer	0.10	-	-	-	-
			Class-8	0.49	0.29	0.10	0.50	1.00
decel	0.1	7.0	Default Passenger	4.50	-	-	-	-
			Cars	3.79	1.58	1.62	3.82	6.29
			SUVs	3.78	1.53	1.71	3.88	6.21
			Trucks	3.66	1.54	1.69	3.66	6.28
			Default Trailer	4.00	-	-	-	-
			Class-8	3.38	1.63	1.35	3.45	6.03
sigma	0.1	1.0	Default Passenger	0.50	-	-	-	-
			Cars	0.34	0.21	0.12	0.27	0.77
			SUVs	0.35	0.21	0.13	0.30	0.77
			Trucks	0.34	0.21	0.12	0.29	0.75
			Default Trailer	0.50	-	-	-	-
			Class-8	0.32	0.17	0.13	0.29	0.63
sigmaStep	0.1	1.0	Default Passenger	0.10	-	-	-	-
			Cars	0.48	0.22	0.19	0.49	0.83
			SUVs	0.49	0.22	0.19	0.48	0.88
			Trucks	0.50	0.23	0.19	0.49	0.90
			Default Trailer	0.10	-	-	-	-
			Class-8	0.50	0.21	0.16	0.53	0.81
speedFactor	0.8	1.8	Default Passenger	1.00	-	-	-	-
			Cars	1.29	0.25	0.96	1.28	1.73
			SUVs	1.28	0.25	0.94	1.27	1.72
			Trucks	1.30	0.25	0.96	1.30	1.72
			Default Trailer	1.00	-	-	-	-
			Class-8	1.31	0.24	1.03	1.32	1.77
tau	0.5	5.0	Default Passenger	1.00	-	-	-	-
			Cars	2.10	1.10	0.89	1.81	4.38
			SUVs	2.12	1.12	0.88	1.85	4.51
			Trucks	2.07	1.11	0.81	1.86	4.35
			Default Trailer	1.00	-	-	-	-
			Class-8	2.50	1.14	0.89	2.42	4.71

[a] Constrained in optimization to a multiple of the simulation step size

Table 5. *Summary statistics for the calibrated W99 model. LB stands for the lower-bound on optimization and UB the upper bound. All parameters are in the naming convention and units presented in the SUMO documentation.*

Parameter	Calibration LB	UB	Cal. Target	Calibrated Parameters μ	σ	$P_{10\%}$	$P_{50\%}$	$P_{95\%}$
actionStepLength [a]	0.1	1.0	Default Passenger	0.10	-	-	-	-
			Cars	0.42	0.28	0.10	0.40	0.90
			SUVs	0.41	0.27	0.10	0.40	0.90
			Trucks	0.41	0.27	0.10	0.30	0.90
			Default Trailer	0.10	-	-	-	-
			Class-8	0.50	0.28	0.20	0.50	1.00
cc1	0.0	5.0	Default Passenger	1.30	-	-	-	-
			Cars	1.51	0.94	0.42	1.36	3.20
			SUVs	1.60	0.92	0.57	1.46	3.28
			Trucks	1.61	0.93	0.49	1.52	3.28
			Default Trailer	1.30	-	-	-	-
			Class-8	2.23	0.95	1.15	2.23	3.84
cc2	0.0	10.0	Default Passenger	8.00	-	-	-	-
			Cars	5.86	2.32	2.89	5.91	9.46
			SUVs	5.98	2.28	2.82	6.01	9.51
			Trucks	5.83	2.41	2.59	5.83	9.64
			Default Trailer	8.00	-	-	-	-
			Class-8	5.83	2.71	1.92	5.93	9.98
cc3	-20.0	0.0	Default Passenger	-12.00	-	-	-	-
			Cars	-10.93	4.69	-17.21	-10.61	-3.43
			SUVs	-11.38	4.75	-18.27	-11.35	-3.08
			Trucks	-10.97	4.75	-17.43	-10.94	-2.97
			Default Trailer	-12.00	-	-	-	-
			Class-8	-10.75	4.30	-16.66	-11.14	-3.41
cc4	-5.0	0.0	Default Passenger	-0.25	-	-	-	-
			Cars	-1.83	1.19	-3.43	-1.71	-0.14
			SUVs	-1.80	1.28	-3.70	-1.66	-0.12
			Trucks	-1.82	1.23	-3.57	-1.70	-0.10
			Default Trailer	-0.25	-	-	-	-
			Class-8	-1.78	1.28	-3.52	-1.69	-0.05
cc5	0.1	5.0	Default Passenger	0.35	-	-	-	-
			Cars	2.00	1.38	0.33	1.74	4.49
			SUVs	2.00	1.32	0.33	1.92	4.47
			Trucks	1.98	1.35	0.32	1.73	4.43
			Default Trailer	0.35	-	-	-	-
			Class-8	2.40	1.26	0.87	2.18	4.49
cc6	0.1	20.0	Default Passenger	6.00	-	-	-	-
			Cars	7.64	4.95	1.05	7.72	17.30
			SUVs	7.30	4.86	1.46	6.72	16.58
			Trucks	7.33	4.85	1.35	6.80	16.78
			Default Trailer	6.00	-	-	-	-
			Class-8	6.81	5.38	0.91	4.84	16.35
cc7	-1.0	1.0	Default Passenger	0.25	-	-	-	-
			Cars	-0.03	0.48	-0.73	-0.07	0.82
			SUVs	-0.10	0.48	-0.75	-0.09	0.79
			Trucks	-0.08	0.49	-0.72	-0.09	0.81
			Default Trailer	0.25	-	-	-	-
			Class-8	-0.01	0.56	-0.77	-0.00	0.93
cc8	0.0	8.0	Default Passenger	2.00	-	-	-	-
			Cars	2.48	1.80	0.68	1.87	6.07
			SUVs	2.56	1.84	0.65	2.03	6.48
			Trucks	2.49	1.84	0.70	1.83	6.44
			Default Trailer	2.00	-	-	-	-
			Class-8	1.97	1.88	0.40	1.38	6.50
cc9	0.0	8.0	Default Passenger	1.50	-	-	-	-
			Cars	4.05	1.98	1.44	3.96	7.19
			SUVs	3.92	2.08	0.96	3.95	7.46
			Trucks	3.87	2.06	1.12	3.74	7.37
			Default Trailer	1.50	-	-	-	-
			Class-8	3.85	2.16	0.66	3.65	7.44
minGap	0.0	20.0	Default Passenger	2.50	-	-	-	-
			Cars	6.14	3.97	1.35	5.41	13.61
			SUVs	6.08	4.21	1.08	5.55	14.14
			Trucks	6.28	4.27	1.11	5.60	14.00
			Default Trailer	2.50	-	-	-	-
			Class-8	7.94	4.87	1.09	7.91	16.82
speedFactor	0.8	1.5	Default Passenger	1.00	-	-	-	-
			Cars	1.09	0.20	0.81	1.08	1.41
			SUVs	1.07	0.20	0.80	1.06	1.42
			Trucks	1.08	0.21	0.80	1.06	1.45
			Default Trailer	1.00	-	-	-	-
			Class-8	1.12	0.20	0.85	1.11	1.42

[a] Constrained in optimization to a multiple of the simulation step size